Acta Pharmaceutica Sinica B 2026;16(3):1762−1768

Chinese Pharmaceutical Association
Institute of Materia Medica, Chinese Academy of Medical Sciences

Acta Pharmaceutica Sinica B

www.elsevier.com/locate/apsb
www.sciencedirect.com

SHORT COMMUNICATION

Aptamers targeting respiratory syncytial virus showed high inhibitory activity by blocking the G protein

Ge Yang[a,c,†], Guangyu Jiang[a,c,†], Xintao Lian[a,c], Boming Cui[a,c], Shuo Wu[a,b,c], Huiqiang Wang[a,c], Haiyan Yan[a,c], Kun Wang[a,c], Rongmei Gao[a,c], Feng Qu[d], Jiandong Jiang[a,b,*], Yuhuan Li[a,b,c,*]

[a]*CAMS Key Laboratory of Antiviral Drug Research, NHC Key Laboratory of Biotechnology for Microbial Drugs, Institute of Medicinal Biotechnology, Chinese Academy of Medical Sciences and Peking Union Medical College, Beijing 100050, China*
[b]*State Key Laboratory of Bioactive Substances and Functions of Natural Medicines, Institute of Medicinal Biotechnology, Chinese Academy of Medical Sciences and Peking Union Medical College, Beijing 100050, China*
[c]*Division for Medicinal Microorganism-Related Strains, CAMS Collection Center of Pathogenic Microorganisms, Chinese Academy of Medical Sciences & Peking Union Medical College, Beijing 100050, China*
[d]*School of Life Science, Beijing Institute of Technology, Beijing 100081, China*

Received 23 July 2025; received in revised form 9 November 2025; accepted 26 November 2025

KEY WORDS

RSV;
Aptamer;
CE-SELEX;
Antiviral activity;
Glycoprotein

Abstract Respiratory syncytial virus (RSV) is a major global health threat, causing severe respiratory disease in infants, the elderly, and immunocompromised individuals—often surpassing the impact of influenza. Yet, effective RSV therapies remain limited. We describe anti-RSV ssDNA aptamers, selected *via* Systematic Evolution of Ligands by Exponential Enrichment (SELEX), that bind the RSV glycoprotein (G) with nanomolar affinity. These aptamer-based therapeutics demonstrated potent antiviral activity against RSV. We further established that the binding domains of these aptamers are critical for their antiviral function. Our findings highlight highly active aptamers as a promising strategy to combat RSV infections.

*Corresponding authors.
E-mail addresses: jiang.jdong@163.com (Jiandong Jiang), yuhuanlibj@126.com (Yuhuan Li).
[†]These authors made equal contributions to this work.
Peer review under the responsibility of Chinese Pharmaceutical Association and Institute of Materia Medica, Chinese Academy of Medical Sciences.

https://doi.org/10.1016/j.apsb.2025.12.027

1. Introduction

Respiratory syncytial virus (RSV) remains a leading global cause of severe respiratory infections in infants, immunocompromised individuals, and the elderly. In 2019 alone[1], RSV caused ∼33 million lower respiratory infections, 3.6 million hospitalizations, and >100,000 deaths in children under 5 years, with persistently high morbidity and mortality through 2022[2]. Among adults ≥65 years, RSV results in 60,000−160,000 annual hospitalizations and 6000−10,000 deaths, posing a substantial public health and economic burden[3-7]. Although four FDA-approved therapies exist—ribavirin (1986), palivizumab (1998), nirsevimab (2023), and clesrovimab (2025)—their limitations are evident: ribavirin faces rising resistance and toxicity, while monoclonal antibodies (mAbs) are prohibitively expensive. Thus, novel, cost-effective RSV therapeutics are urgently needed.

Aptamers, single-stranded DNA/RNA molecules selected *via* SELEX, offer a promising alternative. Combining antibody-like specificity with advantages such as rapid development, low immunogenicity, and tunable chemistry, aptamers have demonstrated broad antiviral potential. Examples include AS1411 (dengue virus)[8], HA-targeting aptamers (influenza)[9], and core protein-specific aptamers (HBV)[10], which disrupt viral attachment, entry, or nucleocapsid assembly. In particular, a variety of aptamers targeting the SARS-CoV-2 have significant broad-spectrum inhibition effects on SARS-CoV-2 infection and replication[11-17]. Therefore, the flexibility of aptamer in target recognition and functional regulation makes it a potential new antiviral therapeutic agent.

Notably, RSV's glycosylated G protein, which mediates viral attachment *via* CX3CR1 or heparan sulfate proteoglycans (HSPGs)[18,19], represents an underexplored therapeutic target. Here, we identify and characterize high-affinity aptamers targeting RSV G protein, elucidating their mechanisms of viral neutralization and inhibition of RSV-long and A2 strains. Our findings not only advance the development of G protein-based RSV therapeutics but also provide a framework for designing broad-spectrum nucleic acid drugs against RSV. This study underscores the potential of aptamers as versatile, safe, and efficient antiviral agents.

2. Materials and methods

2.1. Materials

G proteins (long and A2 strain), RSV F protein, RBD and H1N1 HA were purchased from Sino Biological Inc. Human Serum Albumin was purchased from Sigma−Aldrich LLC. Human IgG Fc fragment was purchased from Abcam. A custom FAM-labeled ssDNA library containing a central 40-nt randomized region flanked by fixed primer sequences (5′-FAM-AGC AGC ACA GAG GTC AGA TG-(N40)-CCT ATG CGT GCT ACC GTG AA-3′) was synthesized by Biological Engineering Technology and Services (Shanghai). Corresponding primers (FAM-labeled forward and unlabeled reverse) were used for amplification.

2.2. CE-SELEX

A Beckman P/ACE MDQ capillary electrophoresis system with fluorescence detection (excitation/emission: 488 nm/520 nm) was used. Separations were performed in a fused silica capillary (75 μm i.d. × 40.0 cm effective length) under conditions of 20 kV voltage, 25 °C, and pH 8.7 borate buffer. The ssDNA library was heat-denatured, refolded, and incubated with diluted G-protein in human saliva matrix at 37 °C for 15 min prior to injection. Data were processed with 32 Karat software.

2.3. Affinity determination via SPR

SPR analysis was performed on a Reichert4 system at 25 °C using a CM5 sensor chip. The target protein was immobilized (∼6000 RU) *via* amine coupling in sodium acetate (pH 4.5). Aptamers were serially diluted (0.002−1 μmol/L) in filtered PBST and injected at 25 μL/min. Real-time binding data were fitted with a 1:1 Langmuir model using BIAevaluation 4.1 to obtain the equilibrium dissociation constant.

2.4. Cell lines and viruses

HEp-2, H460, and A549 cells (ATCC) were cultured in DMEM-based media with 10% FBS and 1% penicillin−streptomycin. RSV Long (VR-26) and A2 (VR-1540) strains were propagated in HEp-2 cells. For replication assays, cells were infected (MOI = 0.01) and treated with aptamers; viral RNA was quantified by qRT-PCR at 24, 48, and 72 hpi. For adsorption/entry inhibition, cells infected at MOI = 0.5 were aptamer-treated and analyzed at 2 hpi. All work followed BSL-2 protocols.

2.5. Western blot

Cell lysates were prepared using M-PER reagent with protease inhibitors. Proteins were separated by SDS-PAGE, transferred to PVDF membranes, blocked with 5% skim milk, and incubated with primary antibodies (β-actin, RSV-G, RSV-N; 1:1000, Cell Signaling Technology) at 4 °C overnight, followed by HRP-conjugated secondary antibodies.

2.6. Quantitative RT-PCR

Total RNA was extracted with the RNeasy Mini Kit and analyzed using TransScript II Green One-Step qRT-PCR SuperMix on an ABI 7500 Fast system. Primer sequences are listed in Supporting Information Table S1.

2.7. Statistical analysis

Data are presented as mean ± standard deviation (SD). Differences were assessed by Student's *t*-test, with $P < 0.05$ considered statistically significant.

3. Results and discussion

3.1. Aptamer selection via pressure-gradient CE-SELEX

Rational aptamer development requires screening conditions that mimic physiological environments to ensure practical transferability. We addressed this critical need through an innovative capillary electrophoresis-SELEX (CE-SELEX) strategy incorporating (Fig. 1A): (1) a human saliva matrix (40- to 10-fold dilution series) to maintain native protein conformation, and (2) a pressure-gradient design progressively increasing stringency (target concentration decent 0.5 → 0.02 μmol/L) (Fig. 1B−E). This dual-parameter optimization enabled efficient isolation of G

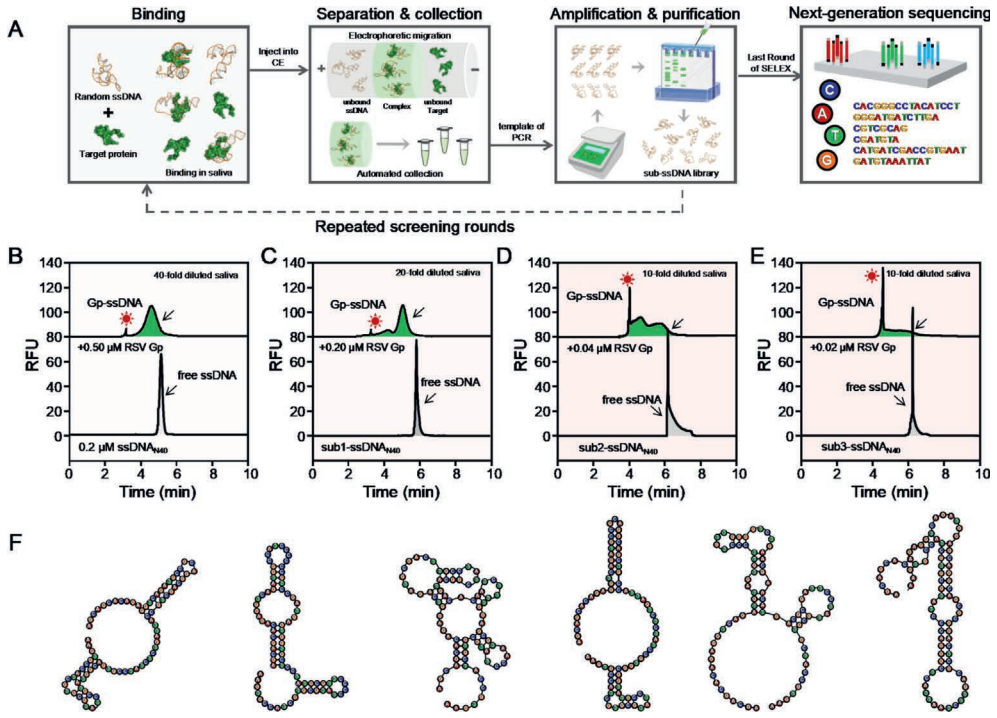

Figure 1 Selection of RSV G protein-specific aptamers (Gp-Apts) *via* CE-SELEX. (A) Schematic of pressure-gradient CE-SELEX. (B−E) CE-LIF electropherograms of selection rounds 1−4, showing enrichment of FAM-labeled ssDNA library (→: unbound ssDNA; ☀: ssDNA-Gp complexes). Only ssDNA signals were detectable due to unlabeled G protein. (F) Predicted secondary structures of six enriched Gp-Apts (UNAFold Web Server).

protein-binding ssDNA complexes (retention time ∼3.12 min) while imposing evolutionary pressure for high-affinity binders. The screening process demonstrated remarkable efficiency, achieving an approximately 10^3-fold enhancement (K_D reduction) within just 4 rounds (Supporting Information Fig. S1). Through high-throughput sequencing analysis of 2000 candidate sequences, we identified six topologically conserved aptamers (Gp-Apts) featuring with complete stem-loop structures (Fig. 1F, Supporting Information Table S2) and characteristic binding motifs (Supporting Information Fig. S2).

3.2. Gp-Apts specifically binds to RSV Gp and recognizes pseudo/inactivated virus

We characterized this novel panel of anti-RSV G protein aptamers (Gp-Apts) with exceptional binding properties, and validated through functional and viral recognition assays. CE-based separation confirmed the formation of stable complex (retention shift: 4.2−6.1 min → 3.0−3.6 min) of the Gp (recombinant protein) and Gp-Apts, indicating strong and uniform binding (Fig. 2A). Further, functional binding of Gp-Apts to virions was evaluated. Viral binding studies demonstrated Gp-Apts recognize both pseudovirus (complex peak: 3.8−4.2 min) and inactivated RSV (complex peak: 2.5 min), despite structural differences (Fig. 2A). Dose-dependent complex formation (R^2 = 0.988) across viral loads (293−18,750 TU/mL) (Supporting Information Figs. S3 and S4), supporting the diagnostic utility of Gp-Apts. These demonstrations of CE-SELEX-derived aptamers binding to full RSV particles, bridging the gap between recombinant protein screening and potential clinical applicability. However, weaker binding to inactivated virus suggests steric hindrance from native viral proteins, highlighting the importance of conformational accessibility in aptamer design. SPR analysis revealed high-affinity interactions of them (K_D = 0.016−92 nmol/L) (Fig. 2B, Supporting Information Table S3). Specificity testing showed no cross-reactivity with serum proteins (HSA, IgG) or unrelated viral antigens (SARS-CoV-2 RBD, H1N1 HA) (Fig. 2C). Additionally, we developed a label-free visual detection system using aptamer-functionalized AuNPs, where target-induced aggregation produced a visible color shift (red → blue) with ∼30 nmol/L detection limit (Gp-Apt2/217) (Supporting Information Fig. S5). Scrambled sequences yielded no false positives, confirming sequence-dependent recognition.

3.3. Evaluation of Gp-Apts' anti-RSV activity and mechanism of action

We systematically assessed the inhibitory effects of six Gp-Apts (Gp-Apt1, -Apt2, -Apt5, -Apt10, -Apt217, -Apt909) against RSV (long strain) infection in Hep2 cells. At 72 hpi, Gp-Apts significantly mitigated RSV-induced cytopathic effects (CPE) in a dose-dependent manner (Supporting Information Fig. S6). qRT-PCR revealed marked reductions in RSV RNA levels at 48 hpi (Fig. 3A), with Gp-Apt2 and Gp-Apt217 exhibiting the highest potency (EC_{50} = 20.50 and 26.35 nmol/L, respectively; Fig. 3C). Western blotting confirmed dose-dependent suppression of G protein expression, further validating antiviral efficacy (Fig. 3E, Supporting Information Fig. S7). Comparable antiviral effects were observed in H460 and A549 cells (Fig. 3D), with no cytotoxicity observed at 5 μmol/L (Supporting Information Fig. S8). The stability of aptamer in bronchoalveolar lavage fluid and fetal bovine serum supports therapeutic efficacy (Supporting

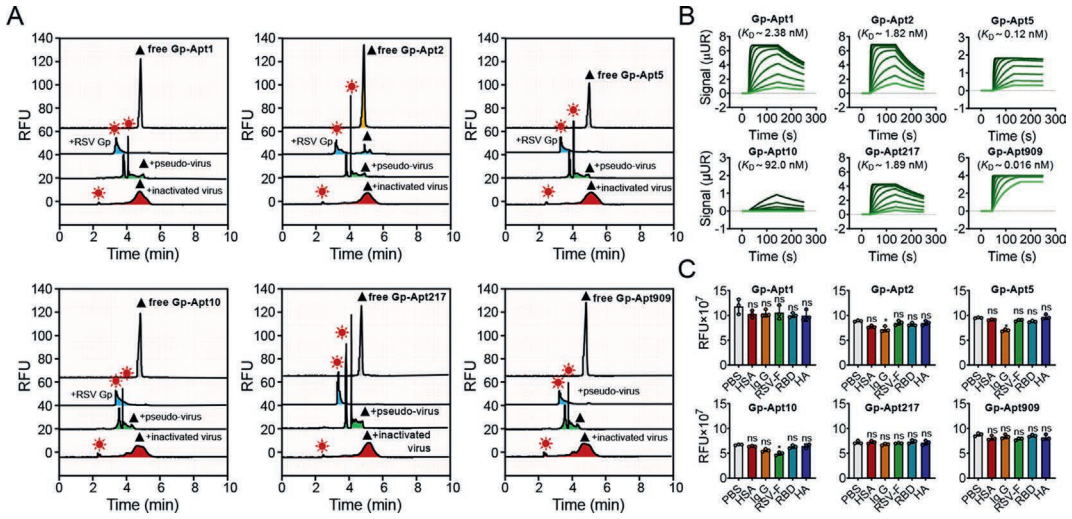

Figure 2 CE-LIF and SPR characterization of Gp-Apt binding to RSV targets. (A) Electropherograms of FAM-labeled Gp-Apts (0.2 μmol/L) and complexes with: (i) recombinant G protein (2 μmol/L), (ii) RSV pseudovirus (75,000 TU/mL), and (iii) inactivated RSV (18,500 PFU/mL). Free aptamers (▲) and complexes (✳) show migration shifts confirming target binding (37 °C, 10 min; $n = 3$). (B) SPR analysis of Gp-Apt affinity for RSV G protein (aptamer gradient: 1 0.5 0.25 0.125 0.062 0.031 0.016 0.008 0.004 0.002 μmol/L). (C) Specificity assessment: FAM-Gp-Apts (0.2 μmol/L) incubated with HSA, anti-RSV-G IgG, RSV F, SARS-CoV-2 RBD, or H1N1 HA (2 μmol/L) and analyzed by CE ($n = 3$). Unbound aptamer peak area (RFU) reflects binding selectivity. Data analyzed by one-way ANOVA (GraphPad Prism 8.0); $^*P < 0.05$.

Information Fig. S9). Cross-strain testing against RSV A2 showed varied inhibition: Gp-Apt2, -Apt5, and -Apt217 retained strong activity (EC_{50} = 19.55−21.12 nmol/L), while Gp-Apt1 and -Apt909 were less effective, and Gp-Apt10 showed no inhibition (Fig. 3B and C). In addition, aptamer exhibit no inhibitory effects against coronaviruses and influenza viruses (Supporting Information Fig. S10). CE confirmed stable complex formation between active Gp-Apts and RSV A2 G protein (Supporting Information Fig. S11), except for Gp-Apt10. Mechanistic studies revealed that Gp-Apts blocked viral attachment (Fig. 3F), and qRT-PCR demonstrated broad suppression of RSV gene expression (F, G, N, P, L, M, NS2) at 48 hpi (Fig. 3G and H). At 1 μmol/L, inhibition exceeded 90%, indicating a consistent, dose-dependent trend across viral transcripts.

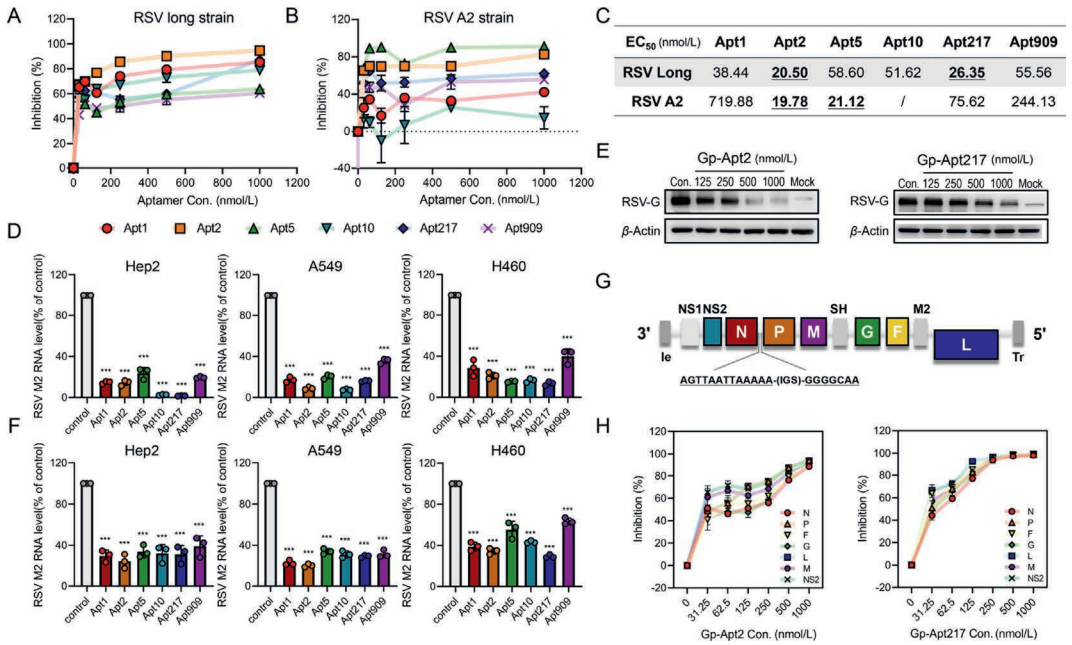

Figure 3 Antiviral activity of Gp-Apts against RSV *in vitro*. (A, B) Inhibition of RSV Long and A2 strains by Gp-Apts at 48 hpi. (C) EC_{50} values of Gp-Apts determined by nonlinear regression (Origin 2018). (D, F) RSV infection and adsorption inhibition by Gp-Apts (1 μmol/L) in Hep2, A549, and H460 cells at 48 hpi ($n = 3$). (E) Western blot analysis of RSV protein expression inhibition at 48 hpi. (G) Schematic of RSV genome. (H) Gp-Apts-mediated reduction of RSV gene expression (F, G, N, P, L, M, NS2). Data analyzed by one-way ANOVA (GraphPad Prism 8.0); $^{***}P < 0.005$.

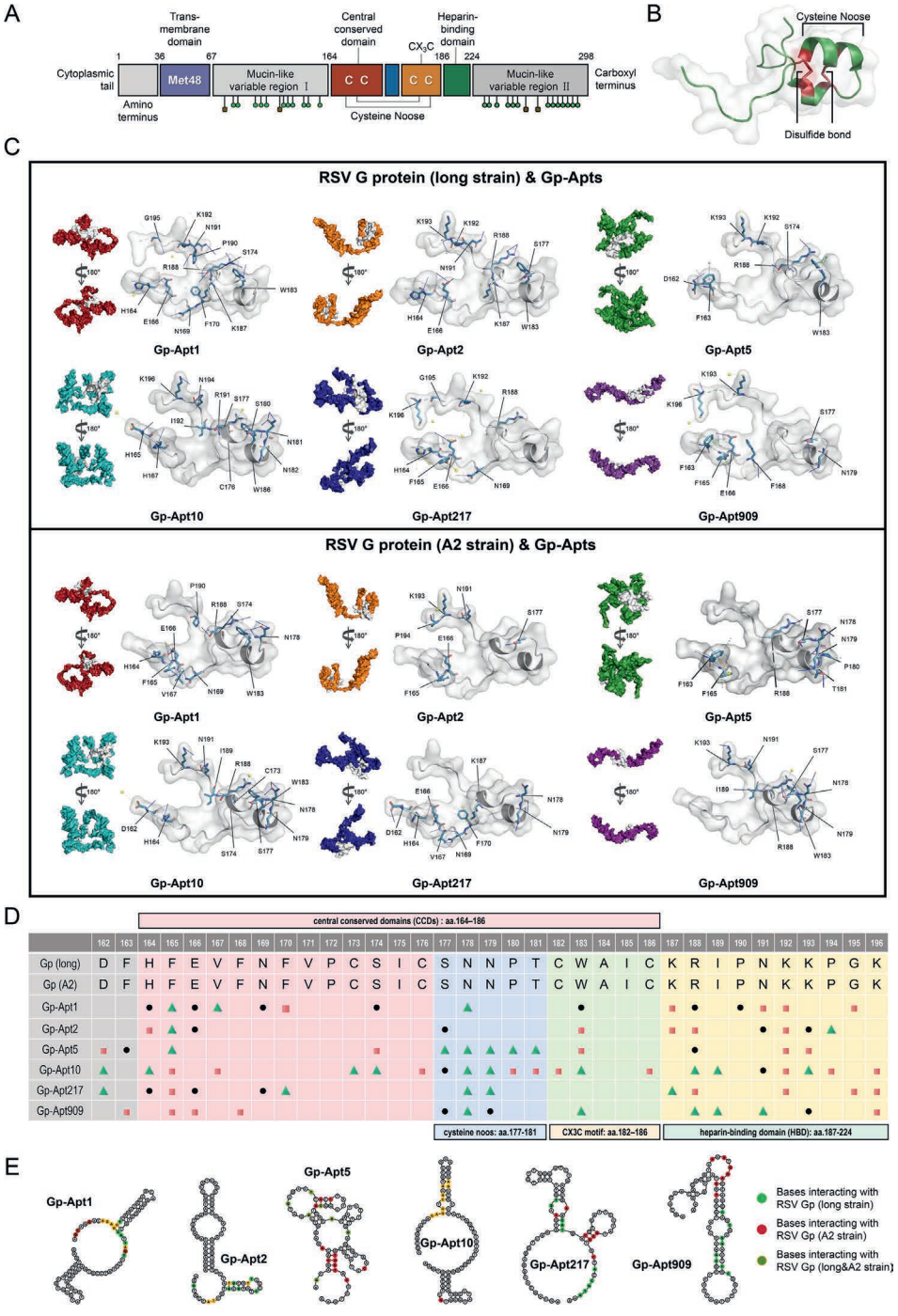

Figure 4 Structural prediction of Gp-Apt binding sites on RSV G protein (Long/A2 strains). (A) Domain architecture of RSV G protein. (B) Predicted G protein structure (AlphaFold). (C) Molecular docking results (HDOCK) showing Gp-Apt binding sites with key residues labeled. (D) Binding site distribution across functional domains (CCDs, cysteine noose, CX3C motif, HBD): ■ (Long strain), ▲ (A2 strain), ● (both strains). (E) Nucleotide residues in Gp-Apts mediating direct contact with G protein.

3.4. Structural basis for broad-spectrum antiviral activity of Gp-Apts

Our structural analyses reveal critical insights into the mechanism of G protein-aptamer interactions (Fig. 4A–C). Molecular docking demonstrated that all Gp-Apts bind to a conserved region (aa 162-196) encompassing both the central conserved domain (CCD) and heparin-binding domain (HBD) of RSV G protein (Fig. 4C). Notably, we identified 11 key amino acid residues (including H164, F165 in CCD and R188, K193 in HBD) that interact with ≥4 different aptamers, representing potential antiviral target sites. The broad-spectrum activity of lead aptamers (Gp-Apt2/5/217) stems from their binding to 12 conserved residues shared between long and A2 strains (Fig. 4D). These structurally rigid aptamers maintain stable interactions through defined stem-loop domains - for instance, Gp-Apt5's "four-leaf clover" structure (Fig. 4E) and

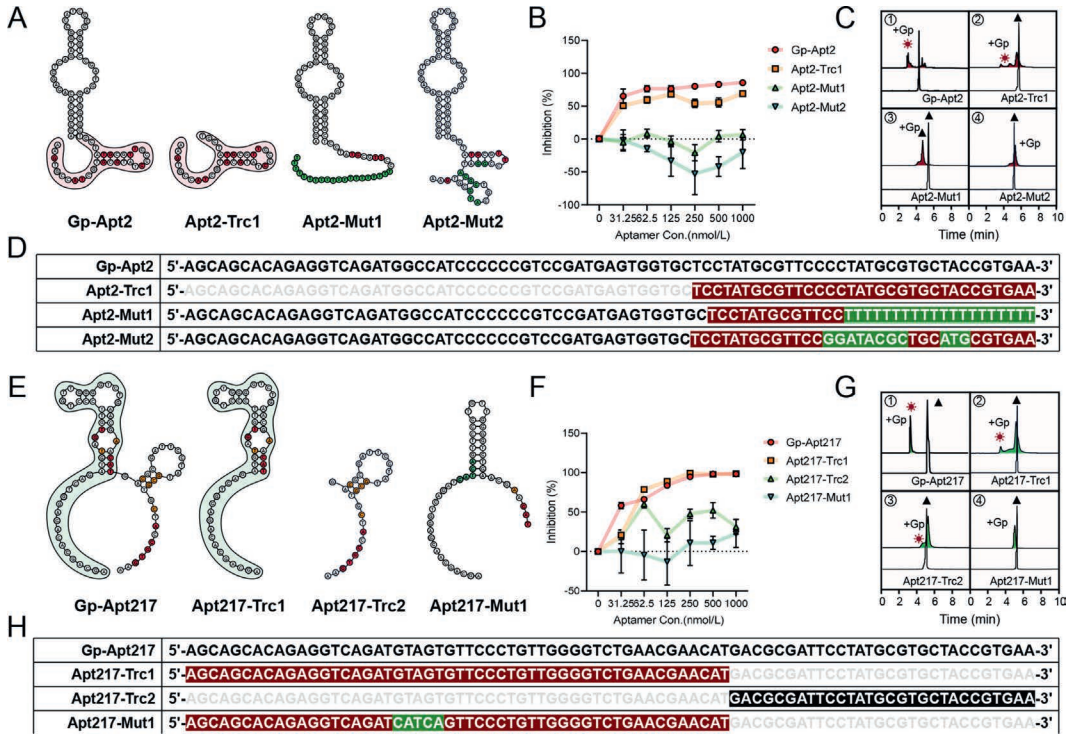

Figure 5 Functional domain characterization of Gp-Apt2 and Gp-Apt217. (A) Schematic of Gp-Apt2 truncation/mutation strategy. (B) Antiviral activity of modified Gp-Apt2 variants against RSV. (C) Binding affinity assessment of Gp-Apt2 variants by CE. (D) Sequence features of Gp-Apt2 variants. (E−H) Parallel analyses for Gp-Apt217 (truncation/mutation design, antiviral activity, CE-based affinity measurement, and sequence information).

Gp-Apt2's 3′-end stem-loop mediate strain-independent binding. Conversely, the flexible, linear-linker containing structures of Gp-Apt1/10 render them susceptible to conformational changes in A2 strain G protein, explaining their reduced efficacy. Molecular dynamics simulations confirmed these aptamers likely bind through induced-fit mechanisms (Supporting Information Fig. S12), making them more sensitive to target variations.

Through aptamer truncation and mutagenesis studies, we elucidated the critical structural determinants governing aptamer antiviral activity (Fig. 5). For Gp-Apt2, the 33-nt binding domain (48T-80A) was both necessary and sufficient for antiviral function (Fig. 5A−C), as demonstrated by: (i) Apt2-Trc1 (48T-80A) maintained full antiviral efficacy and G protein binding capacity, and (ii) Disruption of secondary structure (Apt2-Mut1) or structural inversion (Apt2-Mut2) completely abolished activity. CE analysis confirmed these structural modifications eliminated G protein complex formation (Fig. 5C). In contrast, Gp-Apt217 exhibited a more complex structure-activity relationship. The bipartite binding architecture required cooperation between both stem-loop domains. Apt217-Trc1 (61-nt fragment) retained high activity while Apt217-Trc2 (29-nt) showed 50% reduction (Fig. 5E and F, Supporting Information Table S4). Mutation of the critical GTAGT motif (Apt217-Mut1) led to complete functional loss (Table S4). CE binding assays correlated with antiviral potency, showing reduced affinity for truncated variants (Fig. 5G). These findings reveal two distinct structural mechanisms underlying the antiviral activity of these aptamers: (i) the single-domain Gp-Apt2 operates through a self-contained binding module that determines its functional activity, whereas (ii) the multi-domain Gp-Apt217 requires cooperative interactions between its structural elements for best antiviral function.

4. Conclusions

This study identifies high-affinity DNA aptamers targeting the RSV G protein, demonstrating potent and broad-spectrum antiviral activity *in vitro*. Through an innovative CE-SELEX approach, we isolated aptamers with nanomolar binding affinity that effectively neutralize both Long and A2 strains by blocking viral attachment and suppressing replication (EC_{50} ∼20 nmol/L). Structural characterization revealed conserved binding motifs within the G protein's functional domains, while truncation studies identified critical aptamer regions essential for antiviral function. The aptamers' excellent specificity and biocompatibility underscore their therapeutic potential. Indeed, this study still has additional limitations. Our antiviral evaluation of aptamers was confined to *in vitro* experiments. Based on our preliminary *in vivo* experiments (Supporting Information Fig. S13), the lead aptamer Gp-Apt2-Trac1 demonstrated rapid lung accumulation within 2 h and maintained stability for up to 24 h post intravenous administration, underscoring its potential for treating pulmonary diseases. To further improve targeting efficacy, subsequent studies will focus on structural optimization through the incorporation of lung-targeting motifs and exploration of alternative delivery methods such as pulmonary aerosol administration. Given the complexity of the *in vivo* environment, which may influence the antiviral efficacy of aptamers, further assessment of their potential *in vivo* applications is essential. Additionally, the *in vivo* stability, toxicity, and pharmacokinetics of aptamers are critical areas that require in-depth exploration. Notwithstanding the initial corroboration of the binding site by molecular docking and competitive assays (Supporting Information Fig. S14), its precise elucidation will be the focus of our subsequent work. Currently, the *in vivo* application of aptamer

drugs still encounters numerous challenges, particularly for antiviral aptamers. Translational challenges including *in vivo* stability and potential viral escape mechanisms must be addressed. Our findings not only establish aptamers as promising alternatives to monoclonal antibodies but also provide a framework for developing combination therapies targeting multiple viral proteins. Future studies will focus on efficient screening[20], preclinical validation, and optimization of these nucleic acid therapeutics, for example, developing novel methods for aptamer screening, combining aptamers with drugs for disease treatment[21], thereby advancing their clinical application against RSV.

Acknowledgements

This work was supported by the National Natural Science Foundation of China (82394465, 82394464); The CAMS Innovation Fund for Medical Sciences (CIFMS) (2025-I2M-XHXX-105, 2024-I2M-ZH-012-2402-01, 2021-I2M-1-048, 2021-I2M-1-039, China).

Author contributions

Jiandong Jiang and Yuhuan Li designed research. Ge Yang and Guangyu Jiang performed the majority of the experiments and analyzed results. Xintao Lian, Boming Cui, Shuo Wu, Huiqiang Wang, Haiyan Yan, Kun Wang, Rongmei Gao, and Feng Qu participated in experiments. Ge Yang and Guangyu Jiang wrote the manuscript. Jiandong Jiang and Yuhuan Li reviewed, and edited the paper. All authors have read and approved the article.

Conflicts of interest

The authors declare no conflicts of interest.

Appendix A. Supporting information

Supporting information to this article can be found online at https://doi.org/10.1016/j.apsb.2025.12.027.

References

1. Li Y, Wang X, Blau DM, Caballero MT, Feikin DR, Gill CJ, et al. Global, regional, and national disease burden estimates of acute lower respiratory infections due to respiratory syncytial virus in children younger than 5 years in 2019: a systematic analysis. *Lancet* 2022;**399**:2047−64.
2. Zhang XL, Zhang X, Hua W, Xie ZD, Liu HM, Zhang HL, et al. Expert consensus on the diagnosis, treatment, and prevention of respiratory syncytial virus infections in children. *World J Pediatr* 2024;**20**:11−25.
3. Thompson WW, Shay DK, Weintraub E, Brammer L, Cox N, Anderson LJ, et al. Mortality associated with influenza and respiratory syncytial virus in the United States. *JAMA* 2003;**289**:179−86.
4. Matias G, Taylor R, Haguinet F, Schuck-Paim C, Lustig R, Shinde V. Estimates of mortality attributable to influenza and RSV in the United States during 1997−2009 by influenza type or subtype, age, cause of death, and risk status. *Influenza Other Respir Viruses* 2014;**8**:507−15.
5. Mclaughlin JM, Khan F, Begier E, Swerdlow DL, Jodar L, Falsey AR. Rates of medically attended RSV among us adults: a systematic review and meta-analysis. *Open Forum Infect Dis* 2022;**9**:ofac300.
6. Zheng Z, Warren JL, Shapiro ED, Pitzer VE, Weinberger DM. Estimated incidence of respiratory hospitalizations attributable to RSV infections across age and socioeconomic groups. *Pneumonia (Nathan)* 2022;**14**:6.
7. Hansen CL, Chaves SS, Demont C, Viboud C. Mortality associated with influenza and respiratory syncytial virus in the US, 1999−2018. *JAMA Netw Open* 2022;**5**:e220527.
8. Balinsky CA, Schmeisser H, Ganesan S, Singh K, Pierson TC, Zoon KC. Nucleolin interacts with the dengue virus capsid protein and plays a role in formation of infectious virus particles. *J Virol* 2013;**87**:13094−106.
9. Choi SK, Lee C, Lee KS, Choe SY, Mo IP, Seong RH, et al. DNA aptamers against the receptor binding region of hemagglutinin prevent avian influenza viral infection. *Mol Cells* 2011;**32**:527−33.
10. Zhang Z, Zhang J, Pei X, Zhang Q, Lu B, Zhang X, et al. An aptamer targets HBV core protein and suppresses HBV replication in HepG2.2.15 cells. *Int J Mol Med* 2014;**34**:1423−9.
11. Yang G, Li Z, Mohammed I, Zhao L, Wei W, Xiao H, et al. Identification of SARS-CoV-2-against aptamer with high neutralization activity by blocking the RBD domain of spike protein 1. *Signal Transduct Target Ther* 2021;**6**:227.
12. Yang M, Li C, Ye G, Shen C, Shi H, Zhong L, et al. Aptamers targeting SARS-CoV-2 nucleocapsid protein exhibit potential anti pan-coronavirus activity. *Signal Transduct Target Ther* 2024;**9**:40.
13. Song Y, Song J, Wei X, Huang M, Sun M, Zhu L, et al. Discovery of aptamers targeting the receptor-binding domain of the SARS-CoV-2 spike glycoprotein. *Anal Chem* 2020;**92**:9895−900.
14. Alves Ferreira-Bravo I, DeStefano JJ. Xeno-nucleic acid (XNA) 2′-fluoro-arabino nucleic acid (FANA) aptamers to the receptor-binding domain of SARS-CoV-2 S protein block ACE2 binding. *Viruses* 2021;**13**:1983.
15. Schmitz A, Weber A, Bayin M, Breuers S, Fieberg V, Famulok M, et al. A SARS-CoV-2 spike binding DNA aptamer that inhibits pseudovirus infection by an RBD-independent mechanism. *Angew Chem Int Ed Engl* 2021;**60**:10279−85.
16. Sun M, Liu S, Wei X, Wan S, Huang M, Song T, et al. Aptamer blocking strategy inhibits SARS-CoV-2 virus infection. *Angew Chem Int Ed Engl* 2021;**60**:10266−72.
17. Liu X, Wang YL, Wu J, Qi J, Zeng Z, Wan Q, et al. Neutralizing aptamers block S/RBD-ACE2 interactions and prevent host cell infection. *Angew Chem Int Ed Engl* 2021;**60**:10273−8.
18. Tripp RA, Jones LP, Haynes LM, Zheng H, Murphy PM, Anderson LJ. CX3C chemokine mimicry by respiratory syncytial virus G glycoprotein. *Nat Immunol* 2001;**2**:732−8.
19. Roberts SR, Compans RW, Wertz GW. Respiratory syncytial virus matures at the apical surfaces of polarized epithelial cells. *J Virol* 1995;**69**:2667−73.
20. Yang G, Zhu C, Zhao L, Li L, Huang Y, Zhang Y, et al. Pressure controllable aptamers picking strategy by targets competition. *Chin Chem Lett* 2021;**32**:218−20.
21. Wong KY, Liu Y, Wong MS, Liu J. Cornea-SELEX for aptamers targeting the surface of eyes and liposomal drug delivery. *Exploration* 2024;**4**:20230008.